

which is claimed to be (i) (6). The proposal for an LBHB between Asp¹⁰² and His⁵⁷ is based on criteria (i) and (ii) in studies of several serine proteases, and on the perception that *cis*-urocanic acid mimics the Asp-His H-bond only in nonaqueous solvents.

The LBHB hypothesis states that LBHB formation requires the absence of H-bonding solvents, notably water, and requires matched pK_a values (where K_a is the acid constant) for the heteroatoms involved (6). Here we show experimental facts regarding the Asp-His and *cis*-urocanic acid systems that are inconsistent with these and other key tenets of the LBHB hypothesis as currently framed, namely: (i) the H-bonded ($N^{\delta 1}$ -H) proton is not equally shared between the carboxylate of Asp¹⁰² and $N^{\delta 1}$ of His⁵⁷, but is localized on $N^{\delta 1}$; (ii) the Asp¹⁰²-His⁵⁷ H-bond is not sequestered from water, but is surrounded by freely diffusible water—even in the presence of tightly bound inhibitors; (iii) *cis*-urocanic acid mimics the Asp¹⁰²-His⁵⁷ H-bond not only in organic solvents, but also in water; (iv) the pK_a values of the carboxylic acid and imidazolium groups of *cis*-urocanic acid are not matched under conditions where *cis*-urocanic acid exhibits putative LBHB behavior, but differ by ~ 4 pK_a units; and (v) the bond energies of the Asp-His and *cis*-urocanic acid H-bonds are not > 10 kcal/mol, but are ~ 5 kcal/mol.

A key element of the proposal of Frey *et al.* (6) is that the Asp-His H-bond is low-barrier—that is, equally shared between Asp¹⁰² and His⁵⁷—only when the imidazole ring becomes protonated at $N^{\epsilon 2}$ (+ charged, 4) (Fig. 1A). Were this not the case, the LBHB could be of no advantage to catalysis for reasons Frey *et al.* have outlined. The $N^{\delta 1}$ -H protons in α -lytic protease, chymotrypsin, and other serine proteases resonate at 17 to 18 ppm for protonated His⁵⁷ and at 13.8 to 15 ppm for neutral His⁵⁷ and thus conform to this requirement. In ¹⁵N-labeled α -lytic protease, the $N^{\delta 1}$ -H-bond exhibits spin-coupling constants (J_{NH}) of 80 ± 4 Hz and 90 ± 1 Hz for the protonated and neutral His⁵⁷, respectively (9). Imidazole N-H spin-coupling constants are typically 90 to 98 Hz. Because J_{NH} spin-coupling is a through-bond phenomenon, it is a direct measure of covalent bond character. These J_{NH} values show that the proton is essentially 100% localized on $N^{\delta 1}$ in neutral His⁵⁷ and at least 85% on $N^{\delta 1}$ when His⁵⁷ becomes protonated and engaged in the putative LBHB. N-H spin-coupling is also observed in enzyme-inhibitor complexes, such as that between α -lytic protease and the potent transition-state analog inhibitor MeOSuc-Ala-Ala-Pro-boroVal (inhibition constant $K_i = 6.7 \times 10^{-9}$). His⁵⁷ becomes protonated in

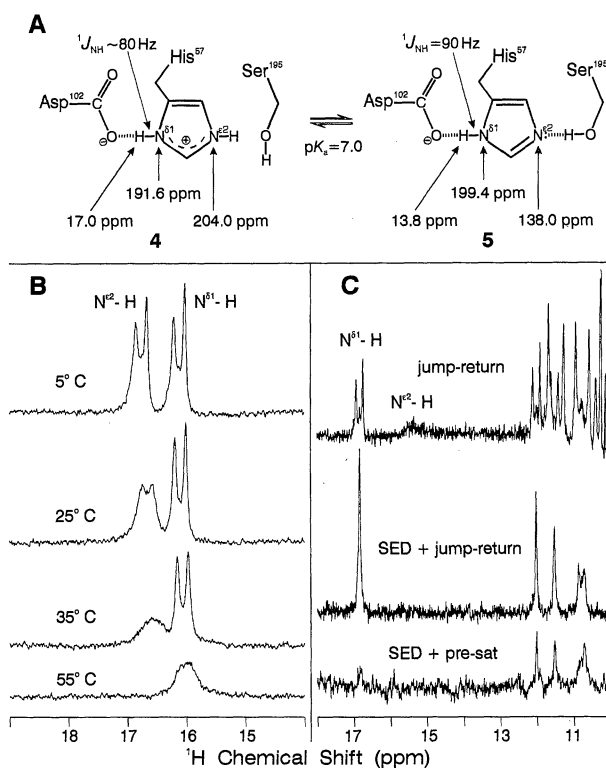
such complexes, as expected for transition-state or tetrahedral intermediate complexes formed with real substrates (10). The ¹⁵N ^{$\delta 1$} -H proton resonance found at 16.1 ppm in the complex (Fig. 1B) exhibits $J_{NH} = 92 \pm 1$ Hz—again showing that the proton remains localized on $N^{\delta 1}$. Halkides and co-workers report a J_{NH} value of 81 Hz for a *Bacillus lentus* subtilisin-Z-Leu-Leu-Phe-trifluoromethyl ketone (Z-LLF-CF₃) complex, indicating $\sim 86\%$ proton localization on $N^{\delta 1}$ of the active site histidine (11).

What magnitude of J_{NH} should be expected for $N^{\delta 1}$ -H of His⁵⁷ if the Asp-His H-bond were low-barrier? The hydrogen bifluoride ion (FHF⁻), widely regarded as the best example of a solution phase, single-well system, exhibits $J_{FH} \approx 120$ Hz in dipolar, aprotic solvents ($\delta = 16.4$ ppm). This coupling is about one-fourth of that observed for HF (476 Hz) (12). By analogy with FHF⁻, we might expect an N-H coupling of ~ 24 Hz

for $N^{\delta 1}$ -H of His⁵⁷ if the H-bond were single-welled. For a double-well system, $J_{NH} = 47$ Hz would be expected from averaging the couplings (0 Hz and 94 Hz) for the two species associated with the potential minima. The observed $N^{\delta 1}$ -H spin couplings in serine proteases indicate that the $N^{\delta 1}$ -H proton can be no more than $15 \pm 8\%$ delocalized when His⁵⁷ is protonated, whether in the resting enzyme or in transition state-like enzyme-inhibitor complexes.

¹⁵N chemical shifts have been shown to be remarkably informative as to the location of imidazole N-H protons (13). In α -lytic protease, $N^{\delta 1}$ and $N^{\epsilon 2}$ resonate at 199.4 and 138.0 ppm, respectively, when His⁵⁷ is neutral, and at 191.6 and 204.0 ppm, respectively, when His⁵⁷ is protonated (Fig. 1A). Pyrrole-like ($>N$ -H), pyridine-like ($>N:$), and protonated, pyrrole-like ($+>N$ -H) ¹⁵N atoms typically resonate at 211, 128, and 202 ± 2 ppm, respectively, in

Fig. 1. (A) ¹⁵N and $N^{\delta 1}$ -H proton chemical shifts, spin-coupling constants, and pK_a value for low- and high-pH forms of resting α -lytic protease. **(B)** His⁵⁷ N-H protons of an α -lytic protease transition-state analog inhibitor complex exchanging with water. "Hard 1-1" ¹H NMR spectra (500 MHz) of uniformly ¹⁵N-labeled α -lytic protease (25) complexed with MeOSuc-Ala-Ala-Pro-boroVal in aqueous solution (pH 4.5) at various temperatures. N-H proton lifetimes, τ , were determined from line-shapes by the slow-exchange approximation, $\tau = 1/(\pi\Delta W)$, where ΔW is excess linewidth attributable to exchange (baseline value of 35 Hz for both peaks obtained from the 5°C spectrum). This leads to lifetimes of $N^{\delta 1}$ -H and $N^{\epsilon 2}$ -H protons, respectively: >42 and >13 ms at 5°C; 42 and 4.5 ms at 25°C; 16 and 1.7 ms at 35°C; and 1.9 and <1.7 ms at 55°C. **(C)** Active site histidine N-H protons of a subtilisin transition-state analog inhibitor complex exchanging more rapidly with water than N-H protons of four other histidine residues. ¹H NMR spectra (500 MHz) of ¹⁵N histidine-labeled subtilisin BPN' (26) complexed with Ac-Ala-Ala-Pro-boroPhe in aqueous solution (pH 5.5) at 25°C. The jump-return spectrum (top) showing ¹H resonances of five of the six subtilisin BPN' histidines (78). The doublet at 16.9 ppm ($J_{NH} = 92$ Hz) and the very broad peak at ~ 15.4 ppm are assigned to the active site histidine (His⁶⁴) $N^{\delta 1}$ and $N^{\epsilon 2}$ protons, respectively. Among the resonances from 10.0 to 12.2 ppm are four additional histidine N-H protons, known to be pH-independent. In additional spectra, systematic reduction in data size down to 2048 data points, recycle delay down to 0.020 s, and repetition times down to 45 ms led to no appreciable loss of signal or noise of the histidine N-H protons (16). The equivalent of a "progressive saturation" T_1 determination, this places an upper limit on the lifetimes of all histidine N-H protons at ~ 15 ms. The ¹⁵N-edited spin-echo difference, jump-return spectrum (SED + jump-return, middle) with ¹⁵N decoupling is simplified, revealing the five ¹H resonances of subtilisin BPN' histidine residues. The SED spectrum with water pre-saturation (SED + pre-sat, bottom) shows that reduction of the active site histidine $N^{\delta 1}$ -H proton resonance at 16.9 ppm is substantially greater than that of the upfield four histidine N-H protons.



aqueous solution (14). H-bonding perturbs these shifts by up to 10 ppm—downfield for >N-H atoms acting as proton donors to carboxylate groups, and upfield for >N: acceptors (13). For α -lytic protease at pH > 9, His⁵⁷ ¹⁵N shifts have been shown to reflect the exclusive presence of the N^{δ1}-H tautomer, **5**, with both ring N atoms engaged in H-bonding; the H-bond to Asp¹⁰² moves N^{δ1} downfield ~10 ppm, whereas the H-bond from Ser¹⁹⁵ moves N^{ε2} upfield ~10 ppm from ¹⁵N shift values expected for the pure N^{δ1}-H tautomer. At pH < 5, where the imidazole ring of His⁵⁷ is protonated, **4**, the H-bond to Asp¹⁰² is reflected in the ~10 ppm downfield displacement of the N^{δ1} resonance from ~202 to 191.6 ppm. Because H-bonding induces chemical shift changes in the same direction, but lower in magnitude, as those induced by protonation or deprotonation, H-bonding effects can be interpreted in terms of partial proton transfer. Thus, the ~10 ppm displacement of N^{δ1}, relative to that for full deprotonation, represents ~14 ± 4% delocalization of the N^{δ1}-H proton (15), a value in good agreement with that determined from ¹J_{NH}.

The LBHB hypothesis requires the serine protease catalytic triad to be sequestered from solvent. Solvent accessibility of N-H groups is often gauged by measuring the rate at which deuterium replaces protons upon dissolution of the protein in D₂O. The N^{δ1}-H proton, however, becomes fully deuterated before an NMR spectrum can be recorded in α -lytic protease and other serine proteases, placing the exchange half-life at <~1.0 min (16). Longitudinal nuclear relaxation time (T₁) measurements on resting α -lytic protease indicate an N^{δ1}-H proton exchange lifetime of <9 ms (16). Transverse nuclear relaxation time (T₂) measurements (lineshape analysis) on

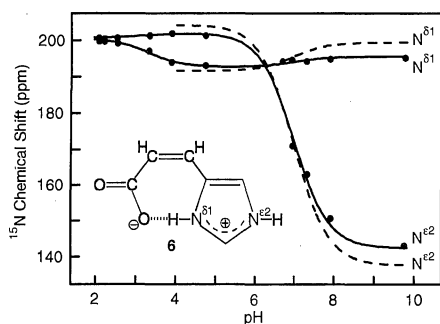


Fig. 2. ¹⁵N chemical shifts versus pH of *cis*-urocanic acid, **6**, are similar to those of His⁵⁷ of α -lytic protease, both in aqueous solution. ¹⁵N shifts for *cis*-urocanic acid (solid line) are given over the pH range 2 to 10, and those of α -lytic protease (dotted line) over the pH range 4 to 10. [Reprinted with permission of Roberts *et al.* (19). Copyright American Chemical Society (1982)]

chymotrypsinogen A indicate an N^{δ1}-H proton exchange lifetime in the millisecond range at 1° to 19°C (17). Such rapid exchange demonstrates the His⁵⁷ N^{δ1}-H proton is highly accessible to solvent in resting serine proteases.

However, it could be argued that occupancy of the active site by substrates or inhibitors might block solvent access sufficiently for LBHB formation. MeOSuc-Ala-Ala-Pro-boroVal, a potent transition-state analog inhibitor of α -lytic protease, occupies subsites S1 to S4, as would a specific substrate. In addition to the Asp-His H-bond (δ = 16.1 ppm), a second putative LBHB (δ = 16.5 ppm) is formed between N^{ε2}-H and the boronyl group in this complex (10). The inhibitor does reduce solvent access, as demonstrated by the narrower linewidth of the N^{δ1}-H proton signal relative to that of resting enzyme (Fig. 1B). Nevertheless, lineshape analysis indicates that the N^{δ1}-H and N^{ε2}-H proton lifetimes are still on the order of milliseconds. In contrast, the lifetime of the bound inhibitor, with a K_i value of 6.7 × 10⁻⁹, is on the order of minutes. Thus, even in this tightly bound inhibitor complex, both imidazole N-H protons of His⁵⁷ are readily accessible to solvent.

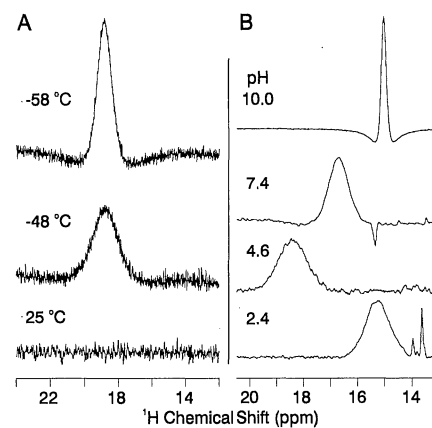
The subtilisin BPN'-Ac-Ala-Ala-Pro-boroPhe (K_i = 1 × 10⁻¹⁰) complex exhibits features similar to those of the α -lytic protease-MeOSuc-Ala-Ala-Pro-boroVal complex, except that exchange of the N^{ε2}-H proton signal with water is more rapid, because its resonance is barely observable at 25°C (Fig. 1C, top) (18). Five of subtilisin's six histidines, the catalytic His and four others, give rise to low-field ¹H signals, an observation aided by ¹⁵N

spectral editing and ¹⁵N decoupling (Fig. 1C, middle). Upon selective irradiation (presaturation) of water (Fig. 1C, bottom), the active site histidine N-H proton resonance essentially disappears, whereas the other four remain visible. Thus, of the five observable histidine residues, the catalytic histidine is the most solvent accessible—even in a complex with a tight-binding transition-state analog inhibitor.

The perception that *cis*-urocanic acid, **6** (Fig. 2), forms an LBHB similar to that of the Asp-His diad only in organic solvents is based on reports that a low-field proton signal is observed in these solvents (17.5 ppm in dimethylsulfoxide, 17.2 ppm in acetonitrile, and 16.9 ppm in acetone), but not in water (6). However, the ability of *cis*-urocanic acid to mimic the Asp-His H-bond is not confined to organic solvents (Fig. 2). The ¹⁵N chemical shift behavior of *cis*-urocanic acid in 100% water at room temperature (19) closely resembles that of His⁵⁷ in α -lytic protease (20) over the entire range of pH stability for the enzyme (~4 to 10). Particularly from pH 4 to 5, the ¹⁵N chemical shifts of *cis*-urocanic acid show the same asymmetry exhibited by His⁵⁷ of α -lytic protease and attributed to the H-bond with Asp¹⁰²—namely, that N^{δ1} resonates ~10 ppm downfield from N^{ε2} and from chemical shifts characteristic of >N-H-type nitrogens.

The above results, showing that aqueous *cis*-urocanic acid is as strongly H-bonded as the Asp-His diad, predict that a low-field N^{δ1}-H proton resonance should be present and suggest that the inability to detect it is due to rapid exchange with solvent. Upon cooling an 85% acetone-*d*₆, 15% H₂O solution of *cis*-urocanic acid at pH 4.4 to

Fig. 3. Low temperatures required for *cis*-urocanic acid to exhibit a low-field N^{δ1}-H proton resonance in water-containing solution. Low-field 400-MHz ¹H NMR spectra are shown for ~0.2 M *cis*-urocanic acid versus pH and temperature in various acetone-*d*₆, water cryosolvent mixtures. *cis*-Urocanic acid was produced by photoisomerization of the *trans* isomer as described (27). pH was measured by immersion of a combination glass electrode and calomel reference (Cole-Parmer, Vernon Hills, IL), standardized with National Bureau of Standards buffers at 25°C. **(A)** ¹H NMR spectra of *cis*-urocanic acid in an 85% acetone-*d*₆, 15% H₂O cryosolvent (pH 4.4) shows the temperature-dependent linewidth of the N^{δ1}-H proton resonance at 18.5 ppm. Upon sample cooling to -48°C, the N^{δ1}-H proton is observable in the aqueous-based solution. With further sample cooling (-58°C) the low-field resonance linewidth decreases, but its chemical shift remains at 18.5 ppm. **(B)** pH dependence of the low-field resonance chemical shift in *cis*-urocanic acid in 90% acetone-*d*₆, 10% H₂O. The N^{δ1}-H proton signal moves from 15.0 ppm at pH 10.0 to 18.5 ppm at pH 4.6, and back to 15.2 ppm at pH 2.4. ¹H spectra were recorded at various temperatures from -43° to -60°C and showed no temperature dependence of chemical shift when referenced to sodium 2,2-dimethyl-2-silapentane-5-sulfonate (DSS) as an internal standard.



-48°C , a low-field signal indeed appears, which sharpens upon cooling to -58°C (Fig. 3A). Furthermore, this signal moves from 15.0 ppm at pH 10.0 to 18.5 ppm at pH 4.6 (Fig. 3B), similar to the Asp-His proton in serine proteases (Fig. 4A).

The LBHB hypothesis requires the carboxylic acid and imidazolium groups of the Asp-His diad or of *cis*-urocanic acid to have equal proton affinities or pK_a values. There is now ample evidence that catalytic histidines in serine proteases have pK_a values of ~ 7.0 (20, 21). Direct pK_a determination for Asp¹⁰², however, has proven elusive. In the absence of this measurement, it could be argued that the pK_a value assigned solely to His⁵⁷ does not reflect the microscopic pK_a of the imidazole group, but rather that of the Asp-His diad unit, within which Asp¹⁰² and His⁵⁷ would have equal pK_a values. As a model of the Asp-His diad, *cis*-urocanic acid affords an opportunity to address the question of the pK_a value of the carboxylate. That a transition between imidazole and imidazolium ion occurs with a pK_a of ~ 7 is strongly supported by ¹⁵N results (Fig. 2) because of the large, characteristic chemical-shift differences ($\Delta\delta$) (13, 20). A separate ionization of the carboxylate with a pK_a of ~ 2.9 can be seen in these curves as the secondary inflection in which N^{δ1} moves from a position characteristic of an H-bonded (191 ppm) to a non-H bonded (~ 201 ppm) $>\text{N-H}$ -type nitrogen as the pH is lowered.

Titration inflections of the imidazole ring protons can be followed under conditions where the N^{δ1}-H proton is visible (Fig. 4A). The $\Delta\delta$'s of the C^{ε1}-H and C^{δ2}-H proton resonances associated with $pK_a = 7.2$ are of the same magnitude and direction as that observed for histidine in aqueous solution at 25°C and is consistent with ionization of the imidazole ring (22). These resonances then move further downfield at the pH 2.9 transition but remain in the range characteristic of protonated imidazole rings. The $\Delta\delta$ of the N^{δ1}-H proton of *cis*-urocanic acid closely parallels that of chymotrypsin (dotted line) over the pH 7.2 transition. The second ionization at pH 2.9 moves the N^{δ1}-H proton of *cis*-urocanic acid 3.3 ppm upfield, effectively reversing the initial downfield movement at $pK_a = 7.2$ that moved this resonance to a position qualifying it as an LBHB by the existing framework.

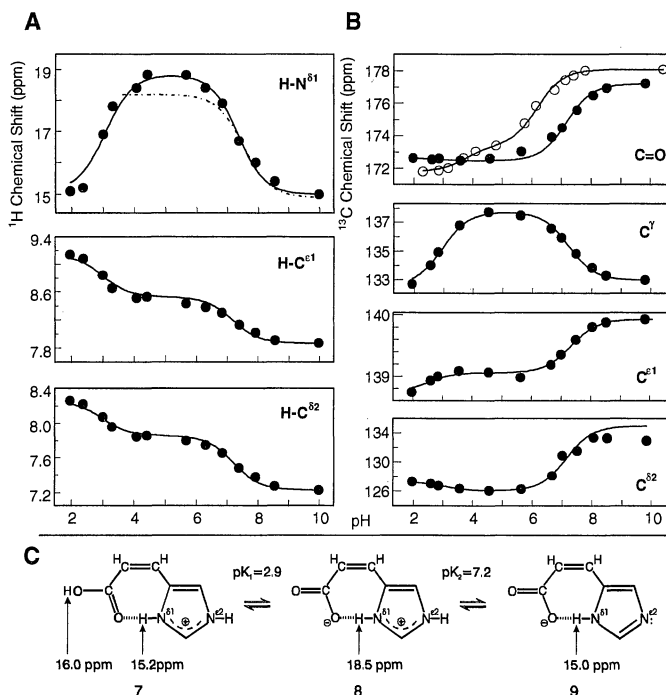
The CO, C^γ, C^{ε1}, and C^{δ2} ¹³C resonances of *cis*-urocanic acid in the acetone-water cosolvent at 25°C respond to the same two pK_a values (7.2 and 2.9) observed in the ¹H and ¹⁵N spectra (Fig. 4B). The behavior of the ¹³CO signal was of special interest, because it might have been expected to provide direct information on the protonation state of the carboxylate group. This ¹³C resonance undergoes a relatively large chemical shift displacement at $pK_a = 7.2$ and a much smaller one at $pK_a = 2.9$. The direction and magnitude of the displacement (3.5 ppm, moving from 176.5 to 173.0

ppm as the group with $pK_a = 7.2$ is protonated) is consistent with displacements observed previously for protonation of carboxylate groups (23). Although this could be construed as support for the LBHB hypothesis, Fig. 4B shows that the ¹³CO signal of *trans*-urocanic acid, which cannot form an intramolecular H-bond, exhibits the same displacement at the imidazole pK_a . The best explanation for the ¹³CO results is transmission of the imidazole protonation effect through the extended conjugated π electron system to the carboxylate group.

All of the NMR results on *cis*-urocanic acid are consistent with the scheme in Fig. 4C. The extreme downfield chemical shift of the ¹H resonance in **8** must be attributed to a strengthening of the H-bond as a result of the coulombic interactions between oppositely charged donor (imidazolium ion) and acceptor (carboxylate) groups—an effect that disappears in **7** (pH < 2.9) and in **9** (pH > 7.2), where either functional group is neutral. This scheme suggests that a second low-field signal should appear at pH < 2.9 , owing to the presence of the protonated carboxylic acid. The spectrum of *cis*-urocanic acid at pH 1.8 and -70°C in 100% acetone-*d*₆ does indeed reveal a second low-field signal at 16.0 ppm (16).

The differences in pK_1 and pK_2 between *cis*- (2.9 and 7.2) and *trans*- (3.7 and 6.2) urocanic acids [ΔpK_a of -0.8 and $+1.0$, respectively, in the acetone-water cosolvent; -0.7 and $+0.9$ in aqueous media (19)] can be attributed directly to the stabilization effect of the intramolecular H-bond (Fig. 4B). The spreading of pK_1 and pK_2 is the result of the H-bond stabilizing the conjugate acid (His⁺) in one equilibrium and the conjugate base (COO⁻) in the other. The average ΔpK_a (0.85 pH units in absolute value) is similar to the ΔpK_a of $+0.8$ units between His⁵⁷ of α -lytic protease and free histidine (20). This corresponds to about 1.2 kcal/mol of stabilization energy at 25°C . Together with the tautomeric equilibrium constant K_T [$>25:1$ (14)] for the stabilization of the N^{δ1}-H tautomer in *cis*-urocanic acid and in His⁵⁷ (19), the overall energy of the H-bond is estimated to be ~ 5 kcal/mol, which is in good agreement with that estimated from Asp¹⁰² mutagenesis experiments (24), but far less than the 10 to 20 kcal/mol of the LBHB hypothesis.

Fig. 4. ¹H and ¹³C chemical shifts of *cis*-urocanic acid versus pH, yielding stepwise pK_a values of a diprotic acid. (A) ¹H NMR chemical shifts for the N^{δ1}-H and ring protons versus pH in 90% acetone-*d*₆, 10% H₂O recorded at low temperatures ranging from -43° to -60°C at 400 MHz. Nonlinear least-squares regression analysis (14) yielded values of $pK_1 = 2.9$ and $pK_2 = 7.2$ for all three protons. The solid lines represent various *cis*-urocanic acid protons, and the dotted line (top) represents the N^{δ1}-H proton of chymotrypsin (28). (B) ¹³C NMR chemical shifts versus pH for the carboxylate and ring carbons of *cis*-urocanic acid (●) and the carboxylate carbon of *trans*-urocanic acid (○) in 90% acetone-*d*₆, 10% H₂O, recorded at 25°C and 100.6 MHz. Nonlinear least-squares analysis of these curves also yielded values of $pK_1 = 2.9$ and $pK_2 = 7.2$. (C) Schematic diagram of *cis*-urocanic acid at low, middle, and high pH values.



REFERENCES AND NOTES

1. F. Hibbert and J. Emsley, *Adv. Phys. Org. Chem.* **26**, 255 (1990).
2. W. P. Jencks, *Catalysis in Chemistry and Enzymology* (Dover, New York, 1987), p. 338.
3. D. J. Millen, A. C. Legon, O. Schrems, *J. Chem. Soc. Faraday Trans. 2* **75**, 592 (1979); A. C. Legon, D. J. Millen, S. C. Rogers, *Proc. R. Soc. London Ser. A* **370**, 213 (1980).

4. R. L. Schowen, in *Mechanistic Principles of Enzyme Activity*, J. F. Liebman and A. Greenburg, Eds. (VCH, New York, 1988), p. 119.
5. W. W. Cleland and M. M. Kreevoy, *Science* **264**, 1887 (1994).
6. P. A. Frey, S. A. Whitt, J. B. Tobin, *ibid.*, p. 1927.
7. J. A. Gerit and P. G. Gassman, *Biochemistry* **32**, 11943 (1993); N. S. Golubev, V. A. Grindin, S. S. Ligal, S. N. Smirnov, *Biochemistry (Moscow)* **59**, 447 (1994); S. N. Smirnov *et al.*, *J. Am. Chem. Soc.* **118**, 4094 (1996); Q. Zhao, C. Abeygunawardana, P. Talalay, A. S. Mildvan, *Proc. Natl. Acad. Sci. U.S.A.* **93**, 8220 (1996); C. S. Cassidy, J. Lin, P. A. Frey, *Biochemistry* **36**, 4576 (1997).
8. Warshel has argued that LBHBs would be anticatalytic in enzymes, whereas Shan *et al.* have examined the energetics of LBHB model systems and failed to find additional stabilization under conditions predicted by LBHB theory [A. Warshel, A. Papazyan, P. A. Kollman, *Science* **269**, 102 (1995); S. O. Shan, S. Loh, D. Herschlag, *ibid.* **272**, 97 (1996); J. P. Guthrie, *Chem. Biol.* **4**, 259 (1996)].
9. W. W. Bachovchin, *Proc. Natl. Acad. Sci. U.S.A.* **82**, 7948 (1985).
10. _____, W. Y. Wong, S. Farr-Jones, A. B. Shenvi, C. A. Kettner, *Biochemistry* **27**, 7689 (1988); C. A. Kettner, R. Bone, D. A. Agard, W. W. Bachovchin, *ibid.*, p. 7682.
11. C. J. Halkides, Y. Q. Wu, C. J. Murray, *ibid.* **35**, 15941 (1996).
12. F. Y. Fujiwara and J. S. Martin, *J. Am. Chem. Soc.* **96**, 7625 (1974); *ibid.*, p. 7632.
13. W. W. Bachovchin, *Biochemistry* **25**, 7751 (1986).
14. S. Farr-Jones, W. Y. L. Wong, W. G. Gutheil, W. W. Bachovchin, *J. Am. Chem. Soc.* **115**, 6813 (1993). ¹⁵N chemical shifts are reported in parts per million upfield of 1.0 M HNO₃, with larger values more upfield. Referencing to liquid NH₃ is obtained by subtraction from 377.5.
15. A downfield displacement of 22.6 ppm in the ¹⁵N chemical shift of N^{δ1} has been reported for subtilisin from *B. lentus* complexed with Z-LLF-CF3 (17). Although this effect was attributed to LBHB formation with ~30% proton transfer, such a fraction is inconsistent with the ¹J_{NH} value of 81 Hz reported by the same authors, which would indicate only ~14 ± 8% delocalization with respect to the average imidazole value of 94 ± 4 Hz. The inconsistency may be attributable to incomplete characterization of the system, including ¹⁵N shifts for both N^{δ1} and N^{ε2} in the complex and resting enzyme.
16. E. L. Ash, J. L. Sudmeier, W. W. Bachovchin, unpublished data.
17. J. L. Markley and W. M. Westler, *Biochemistry* **35**, 11092 (1996).
18. W. W. Bachovchin, *Stable Isotope Applications in Biomolecular Structure and Mechanisms*, J. Trehwella, T. A. Cross, C. J. Unkefer, Eds. (Los Alamos National Laboratory, Los Alamos, NM, 1994), p. 41; R. M. Day, thesis, Tufts University, Boston, MA (1995).
19. J. D. Roberts, C. Yu, C. Flanagan, T. R. Birdseye, *J. Am. Chem. Soc.* **104**, 3945 (1982).
20. W. W. Bachovchin and J. D. Roberts, *ibid.* **100**, 8041 (1978).
21. J. L. Markley, *Biological Applications of Magnetic Resonance* (Academic Press, New York, 1979); F. Sakiyama and Y. Kawata, *J. Biochem.* **94**, 1661 (1983).
22. J. L. Markley, *Acc. Chem. Res.* **8**, 70 (1975).
23. W. J. Horsley and H. Sternlicht, *J. Am. Chem. Soc.* **90**, 3738 (1968).
24. C. S. Craik, S. Rocznik, C. Largman, W. J. Rutter, *Science* **237**, 909 (1987); P. Carter and J. A. Wells, *Nature* **332**, 564 (1988).
25. Uniformly ¹⁵N-labeled (>96%) α-lytic protease (E.C. 3.4.21.12) was expressed by fermentation of wild-type *Lysobacter enzymogenes* in Celtone-N (Martek Biosciences), a medium containing ¹⁵N-enriched peptides and amino acids, which was supplemented with glucose and various salts. Purification of α-lytic protease and assay of enzymatic activity was accomplished as described (18).
26. Expression of ¹⁵N histidine-labeled subtilisin BPN'97 was accomplished by fermentation of a histidine

auxotrophic strain of *Bacillus subtilis* DB104 in a minimal medium containing histidine labeled with ¹⁵N at both ring nitrogens (18). Purification of labeled subtilisin BPN'97 was accomplished by dialysis into a 10 mM tris solution (pH 6.0) and subsequent passage over a CM52 cellulose ion-exchange column, with elution of the protein in 0.01 M MES and 0.1 M KCl. Enzyme activity was measured by a colorimetric assay with the substrate succinyl-L-Ala-L-Ala-L-Pro-L-Phe-paranitroanilide (18).

27. I. Santucci, thesis, Flinders University of South Australia, Bedford Park, South Australia (1995).
28. G. Robillard and R. G. Schulman, *J. Mol. Biol.* **71**, 507 (1972).
29. We thank R. M. Day for supplying the subtilisin BPN' NMR sample, C. A. Kettner for supplying boronic acid inhibitors, and N. I. Krinsky for helpful discussions. Supported in part by NIH grant GM27927.

25 July 1997; accepted 3 October 1997

Inhibition of Brain G_z GAP and Other RGS Proteins by Palmitoylation of G Protein α Subunits

Yaping Tu, Jun Wang, Elliott M. Ross*

Palmitoylation of the α subunit of the guanine nucleotide-binding protein G_z inhibited by more than 90 percent its response to the guanosine triphosphatase (GTPase)-accelerating activity of G_z GAP, a G_z-selective member of the regulators of G-protein signaling (RGS) protein family of GTPase-activating proteins (GAPs). Palmitoylation both decreased the affinity of G_z GAP for the GTP-bound form of Gα_z by at least 90 percent and decreased the maximum rate of GTP hydrolysis. Inhibition was reversed by removal of the palmitoyl group by dithiothreitol. Palmitoylation of Gα_z also inhibited its response to the GAP activity of Gα-interacting protein (GAIP), another RGS protein, and palmitoylation of Gα_{i1} inhibited its response to RGS4. The extent of inhibition of G_z GAP, GAIP, RGS4, and RGS10 correlated roughly with their intrinsic GAP activities for the Gα target used in the assay. Reversible palmitoylation is thus a major determinant of G_z deactivation after its stimulation by receptors, and may be a general mechanism for prolonging or potentiating G-protein signaling.

The α subunits of most heterotrimeric G proteins are modified by irreversible lipid amidation of the NH₂-terminus and by addition of a palmitoyl thioester at a nearby, conserved cysteine residue (1, 2). Unlike myristoylation, palmitoylation of Gα subunits is reversible, and bound palmitate turns over rapidly in cells. Although virtually nothing is known of the enzymes that catalyze addition and removal of palmitate, palmitate turnover on G-protein α subunits appears to be regulated coordinately with their activation and deactivation. In the case of Gα_s (3, 4) and Gα_q (5), substantial depalmitoylation occurs upon receptor-promoted activation, and repalmitoylation of Gα_s coincides at least roughly with deactivation (3). Treatment with cholera toxin, which prolongs activation of G_s by blocking hydrolysis of bound GTP, also promotes turnover of bound palmitate (6). Conversely, palmitate turnover on Gα_i and Gα_o is decreased by coexpression of excess Gβγ, which inhibits activation (6, 7).

Palmitoylation is involved in anchoring Gα subunits to the membrane or specifying

their membrane localization, or both (1–4, 7–9), by increasing their intrinsic hydrophobicity and, at least for Gα_s, by increasing affinity for Gβγ (7). Mutation of the palmitoylated cysteine of Gα_z to alanine also potentiated inhibition of adenylyl cyclase in transfected cells (9). Palmitoylation has not yet been linked to alteration of a specific G-protein signaling function, however. It is not required for interaction of Gα subunits with receptors or effectors *in vitro* (10), and no effect of palmitoylation on the binding or hydrolysis of guanine nucleotides has been reported. Mutation of the palmitoylatable cysteine residue in Gα_q or Gα_s inhibited signaling (11), but signaling was potentiated by the same mutation in Gα_z or Gpa1p, the major Gα subunit in *Saccharomyces cerevisiae* (9, 12). Although palmitoylation may be responsible for such variable effects on different Gα subunits, these results may also arise from effects of mutating the cysteine residue that are unrelated to palmitoylation (10).

We describe the inhibition of the effects of the major G_z GTPase activating protein, G_z GAP, by palmitoylation of Gα_z. G_z is a relatively rare member of the G_i family that is found in brain, platelets and adrenal medulla, and is therefore suspected to be involved in regulation of secretion (13). Isolated Gα_z hydrolyzes bound GTP slowly,

Department of Pharmacology, University of Texas Southwestern Medical Center, 5323 Harry Hines Boulevard, Dallas, TX 75235–9041, USA.

*To whom correspondence should be addressed.